Application note

In situ measurement of CO_2 by FTIR for accelerated polymer aging evaluation

Authors

Jing Xu, Jessica Deng, and Rui Chen, PhD.,
Thermo Fisher Scientific

Introduction

Polymer aging refers to the degradation process that occurs in polymer materials over time when exposed to environmental stress factors such as heat, light, oxygen, moisture, and mechanical stress. These stressors lead to changes in polymers' physical and chemical properties, and ultimately affect their performance and durability. A thorough understanding of polymer aging provides insight to material lifetime, long-term stability, and durability. This aides in the design of materials with better resistance to aging as well as the development of accelerated aging tests for quality control and product certification.

To reduce the time needed to estimate the lifetime of materials, accelerated polymer aging studies focus on degradation chemistry to determine activation energies, thereby predicting degradation rates under normal use conditions. There are numerous accelerated aging methods for durability evaluation defined by the International Organization for Standardization (ISO). For examples, the ISO 4665 and ISO 4892 procedures utilize laboratory lamps to simulate external environments under sunlight (weathering). The ISO 2578 and ISO 11346 methods employ temperatures higher than those under actual use conditions. For accelerated aging studies within a short evaluation time, it is critically important to accelerate degradation using more than one type of stress factor.[1]

Overall degradation kinetics can be tracked by monitoring changes in materials' physical properties and/or chemical properties. Fourier transform infrared spectroscopy (FTIR) has been extensively used in polymer aging studies, primarily for identifying oxidation products and quantifying oxidation extent.[2] Measurements of CO_2 evolution in polymer degradation have also been reported.[3-7] Volatile gases, most commonly CO, CO_2 and H_2O, have been used to probe early-stage degradation where only low conversion or minor degradation levels are encountered.[3] Gas evolution chemical pathways are intrinsic parts of the dominant degradation chemistry. For example, the oxidative degradation of polyethylene (PE) and polypropylene (PP) involves hydroperoxide intermediates, which are unstable to both heat and UV light, followed by alkoxy radicals and scission reactions to form carbonyl groups and end-alkyl radicals. Subsequent reaction of the end-alkyl radicals leads to the formation of CO_2.[7-8] The rate of CO_2 generation directly correlates to the aging activation energy described by the Arrhenius equation (Equation 1), where k is the rate of CO_2 generation, A is the pre-exponential factor, E_a is the activation energy, R is the molar gas constant, and T is the absolute temperature.

$$k = Ae^{\frac{E_a}{RT}}$$

Equation 1.

In this application note, the quantitative determination of the aging activation energy for PP and PE, through the *in situ* FTIR measurements of CO_2 evolution inside an accelerated aging apparatus, is demonstrated.

thermo scientific

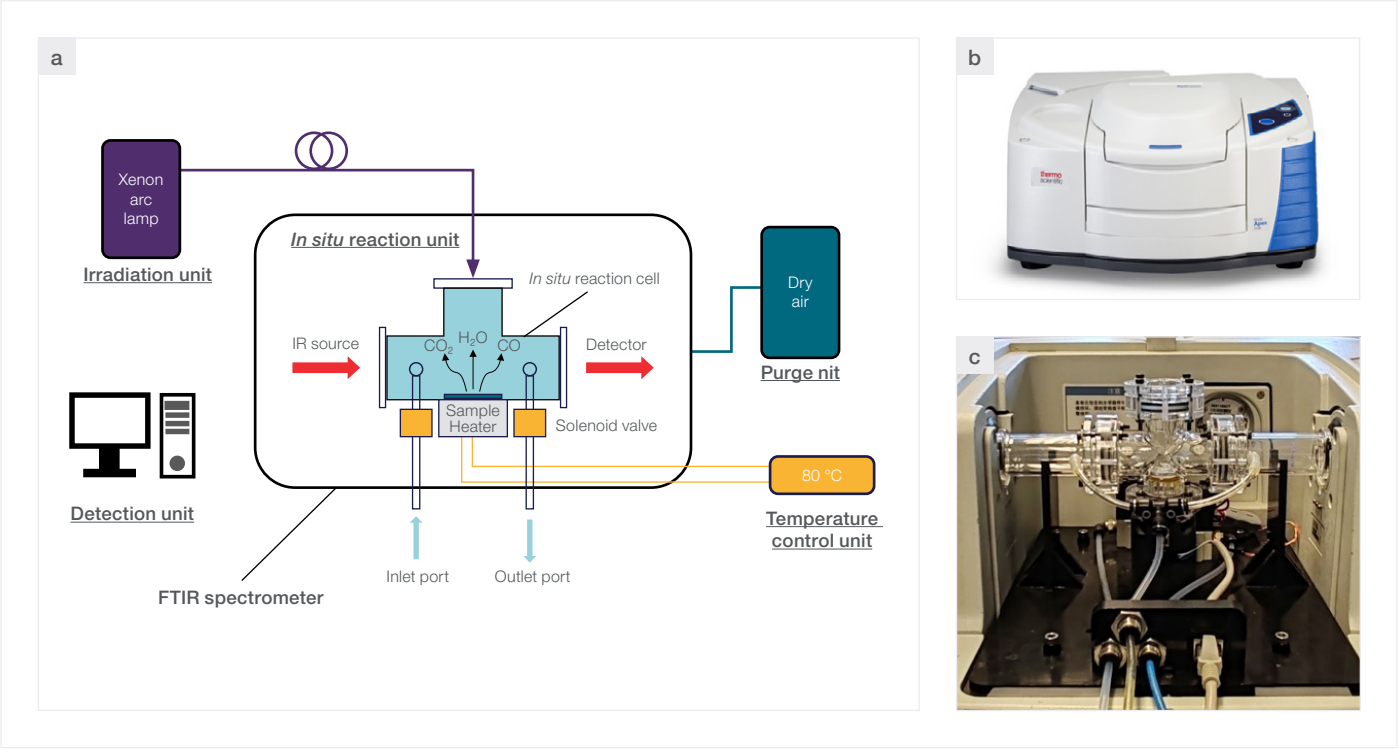

Figure 1. (a) The schematic illustrating the working principles of StablEval-30 for accelerated aging studies; (b) photo of a Thermo Scientific™ Apex™ FTIR Spectrometer; and (c) photo of a StablEval-30 apparatus inside the sample compartment of an Apex FTIR spectrometer.

Experimental

All experiments were performed using a Thermo Scientific™ Nicolet™ iS20 FTIR spectrometer, with an accelerated aging apparatus, StablEval-30, placed in the main sample compartment (Figure 1). Note that since the experiments, the next-generation Thermo Scientific™ Nicolet™ Apex™ FTIR spectrometer (Figure 1b) was launched to succeed the iS20 FTIR spectrometer, with enhanced performance and a new software platform, Thermo Scientific™ OMNIC™ Paradigm Software, for data acquisition and analysis. The accelerated aging apparatus StablEval-30 enables independent control of temperature, humidity, UV irradiation, and oxygen concentration, thus offering different combinations of these environmental factors to simulate different use conditions. The apparatus also serves as a gas cell that allows *in situ* measurements of the gases generated during degradation.[9] The iS20 was equipped with a liquid nitrogen-cooled Mercury Cadmium Telluride (LN2-MCT) detector. Transmission mode was used for spectral collection with a spectral resolution of 4 cm^{-1} and 32 scans were co-added for each spectrum. The Series function of the OMNIC software was used for data acquisition. The peak area of the spectra region 2,253-2,433 cm^{-1} was used to track the CO_2 evolution.

Thin films of polymer samples were placed in the sample tray inside the StablEval-30 reaction chamber. UV irradiation using a xenon lamp was maintained at 90 mW/cm^2 at 365 nm; the spectral distribution curve of the xenon lamp agrees well with that of sunlight. The apparatus was purged with dry air at a flow rate of 5 L/min for a minimum of 20 minutes prior to each aging test. The total duration of each accelerated aging test was 240 minutes and the FTIR measurements were taken at 5 minute intervals. For each test, the system was first equilibrated for 30 minutes (T-0 to T-30) until the FTIR background stabilized. The aging settings were then applied at T-30. The UV irradiation was shut off at T-210 and the data acquisition was stopped at T-240.

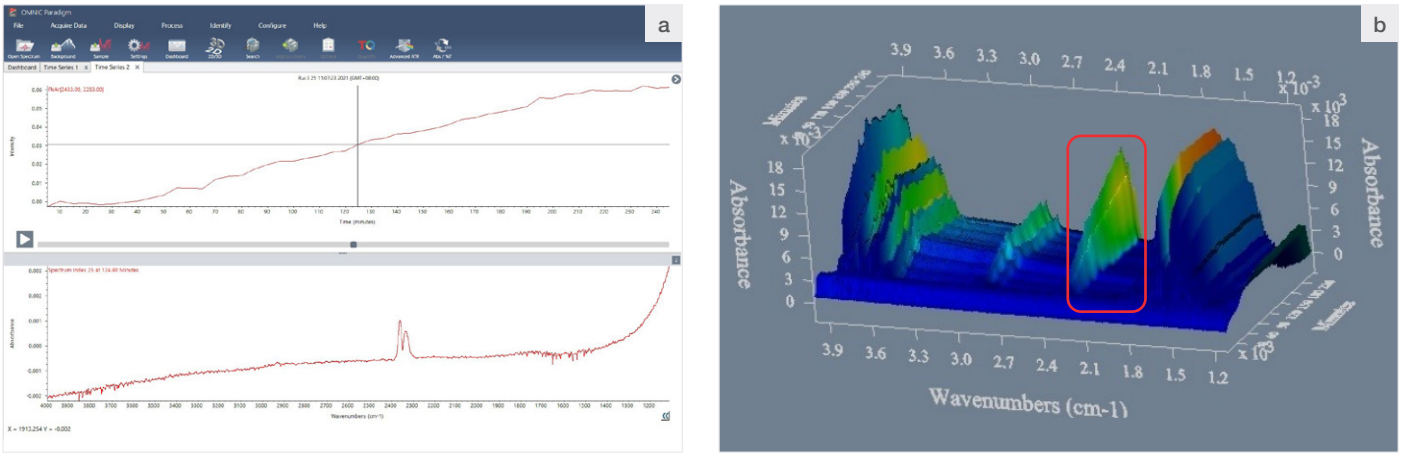

Figure 2. (a) Representative CO_2 peak area profile and FTIR spectrum of an accelerated ageing test; and (b) 3-D representation of an accelerated ageing test. The area inside the red rectangle shows the CO_2 evolution over the course of the experiment.

Results and Discussion

Figure 2a shows a representative peak area profile (top) constructed based on the peak area of CO_2 from the FTIR spectrum (bottom). Figure 2b is a 3-D representation depicting a complete aging experiment, in which the CO_2 evolution is highlighted in the red rectangle. At a quick glance, the CO_2 peak area increases steadily between T-30 and T-210 when the heating and UV irradiation were on. This rise portion of the peak area profile reflects the combined contributions from both photo- and thermo-oxidation. The profile plateaus after T-210 when the UV irradiation was turned off, suggesting that there is no appreciable CO_2 generated in the absence of UV light. Determination of the exact degradation pathways requires a more rigorous understanding of the materials under investigation and more controlled experiments; such testing is outside the scope of this application note. The observations here nonetheless highlight the synergistic impact of UV irradiation and heating on the overall oxo-degradation.

The results of the accelerated aging experiments for PP and PE at six different temperatures are summarized in Figures 3. These results demonstrate that (1) CO_2 was evolved from both PP and PE; (2) more CO_2 was evolved from PP than from PE; and (3) the rate of CO_2 generation, indicated by the slopes of the peak area profile between T-30 and T-210, increases as temperature increases. High temperatures impart thermal energy to polymer molecules, increasing their kinetic energy. This increased kinetic energy allows polymer chains to move more freely, making them more susceptible to bond breaking. At elevated temperatures, the combination of increased thermal energy and enhanced reactivity of polymer molecules leads to accelerated polymer degradation.

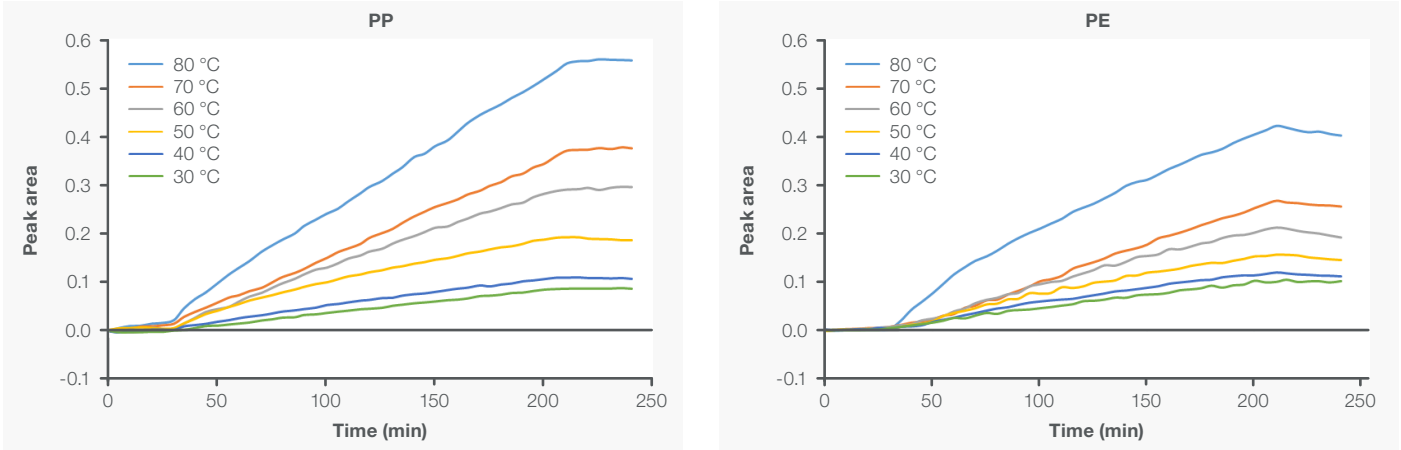

Figure 3. The CO_2 peak area profiles for PP and PE at six different temperatures.

Taking the natural logarithm of both sides of the Arrhenius equation (shown in Equation 1) leads to the following (Equation 2):

$$\ln k = \ln A - \frac{E_a}{RT} = -\frac{E_a}{R} \times \frac{1}{T} + \ln A$$

Equation 2.

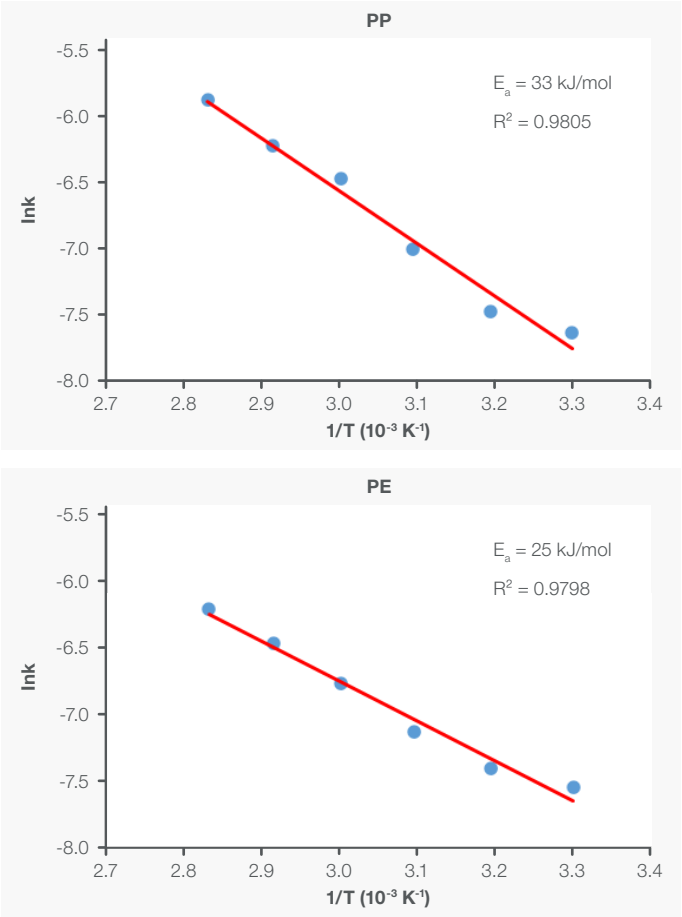

Figure 4. The Arrhenius plot and the activation energy for PP and PE.

There is a simple linear relationship between $\ln k$ and $\frac{1}{T}$. The slope of this linear relationship is $-\frac{E_a}{R}$, from which the Arrhenius activation energy E_a can be calculated. Figure 4 shows the Arrhenius plots ($\ln k$ vs. $\frac{1}{T}$) for PP and PE, with excellent linearity coefficients (R^2) in both cases. The calculated activation energies are 33 kJ/mol for PP and 25 kJ/mol for PE, respectively, with good agreements with the reported values in literature.[10-11] Note that the calculated activation energies here are largely phenomenological, because multiple reactions are occurring simultaneously. Caution should be exercised when interpreting and comparing the values.

Conclusions

In this application note, the *in situ* measurements of CO_2 evolution resulting from accelerated aging of PP and PE by FTIR, are described. The CO_2 evolution profiles at different temperatures exhibit Arrhenius behavior, from which the aging activation energies are calculated. The *in situ* measurements of CO_2 were enabled by a specially constructed gas cell that allows simultaneous UV irradiation, heating, and IR interrogation. FTIR shows great sensitivity in detecting trace level gaseous degradation products and is well suited to investigate early-stage polymer degradation. Each accelerated aging test was completed in less than five hours, much shorter than conventional accelerated tests. This experimental approach holds great promise in supplementing existing accelerated aging tests to better understand and evaluate aging behavior of a wide range of polymer materials.

References

1. Funabashi M., Ninomiya F, Oishi A, Ouchi A, Hagihara H, Suda H, Kunioka M, *Journal of Polymers*, Volume 2016, Article ID 8547524.
2. X. Liu, C. Gao, P. Sangwan, L. Yu, Z. Tong, *J. Appl. Polym. Sci.* 2014, DOI: 10.1002/APP.40750
3. Giron, NH, Celina, *Polym Degrad Stab.*2017;145:93-101.
4. Christensen PA, Dilks A, Egerton TA, Temperley J. *J Mater Sci*, 1999;34:5689-5700.
5. Christensen PA, Dilks A, Egerton TA, Temperley J. *J Mater Sci*, 2000;35:5353-5358.
6. Christensen PA, Dilks A, Egerton TA, Lawson J, Temperley J. J *Mater Sci*, 2002;37:4901-4909.
7. C. Jin, P.A. Christensen, T.A. Egerton, E.J. Lawson, J.R. White, *Polym Degrad Stab.* 91 (2006), 1086-1096
8. Delprat P, Duteurtre X, Gardette J-L. *Polym Degrad Stab.*1995;50:1-12.
9. An Z., Yang R., *Acta Polymerica Sinica*, 2021,52(2):196-203. DOI:10.11777/j.issn1000-3304.2020.20150.
10. Cruz-Pinto JJC, Carvalho MES, Ferreira JFA, *Die Angewandte Makromolekulare Chemie*.1994, 216(1).113-133. DOI:10.1002/apmc.1994.052160108.
11. Jiri T, Zlata V. *Polymer Testing*. 2014, 36. 10.1016/j.polymertesting.2014.03.019.

Learn more at **thermofisher.com/polymer**